

Computer Analysis of Transient Voltages in Large Grounding Systems

Leonid D. Grcev, Member, IEEE

Faculty of Electrical Engineering, University "St. Kiril & Metodij"

Skopje, Republic of Macedonia

Abstract—A computer model for transient analysis of a network of buried and above ground conductors is presented. The model is based on the electromagnetic field theory approach and the modified image theory. Validation of the model is achieved by comparison with field measurements. The model is applied for computation of transient voltages to remote ground of large grounding grid conductors. Also computation of longitudinal and leakage currents, transient impedance, electromagnetic fields, and transient induced voltages is possible. This model is aimed to help in EMC and lightning protection studies that involve electrical and electronic systems connected to grounding systems.

KEYWORDS - Grounding grids, Transient voltages, Computer modeling, EMC, Lightning protection.

I. INTRODUCTION

Extended meshed networks of buried conductors are considered as the most effective solution for grounding systems of large substations and plants. The primary goal of such grounding systems is to ensure the safety of personnel and prevent damage of installations. Their secondary goal is to provide common reference voltage for all interconnected electrical and electronic systems [1].

A grounding system that is equipotential is a theoretical concept applicable in static case. In practical cases the electromagnetic induction makes the voltage between any two points greater than zero. Such local inequalities of the reference voltage and conducted disturbances can be a cause of malfunction and destruction of components in electrical and electronic systems connected to the

grounding system. As a consequence, electromagnetic compatibility (EMC) studies require the knowledge of the spatial and temporal distribution of voltages along the grounding systems in case of lightning and power system faults.

Estimation of the transient performance of grounding grids has been dealt with by many researchers [2-11]. Except [2,3], that are based on the empirical approach, all other approaches are analytical. Basically three different analytical approaches have been used, based on: circuit theory [4,7], transmission line theory [5,6,10] and electromagnetic field theory [8,9,11]. Although, circuit and transmission line models can probably be used for computation of impedance, the electromagnetic models look more appropriate for computation of voltages between two arbitrary points. Computation of voltages between points at the earth's surface above a mesh-type grounding system is described in [9]. Possibility of computation of voltage to remote reference ground of a point at the surface of the conductor is described in [8].

In this paper a computer model for time-harmonic and transient analysis of a network of buried and above ground conductors is described. The analytical model is based on exact closed-form expressions for fields and electromagnetic coupling between elements of the system, thus avoiding numerical treatments typical for other methods. Such accurate modeling enables computation of very near fields, even on the surface of the conductor. On the other side, this enables computation of voltages between points at the surface of the conductor. The computer model is computationally efficient and can be applied to large structures. The only simplification is application of the modified image theory. This limits the domain of applicability of the model to frequencies lower than few MHz, which is suitable for analysis of responses to typical lightning and similar impulses.

II. ANALYTICAL MODEL

The transient problem is first solved by a formulation in the frequency domain. The time domain response is then obtained by application of a suitable Fourier inversion technique [8].

95 SM 363-2 PWRD A paper recommended and approved by the IEEE Substations Committee of the IEEE Power Engineering Society for presentation at the 1995 IEEE/PES Summer Meeting, July 23-27, 1995, Portland, OR. Manuscript submitted December 27, 1994; made available for printing May 3, 1995.

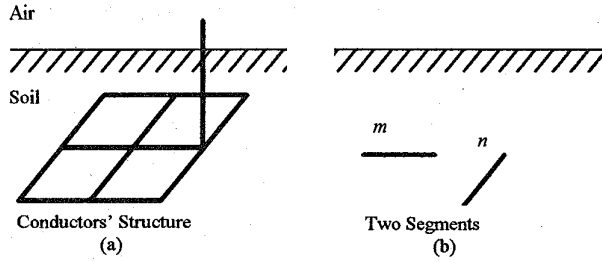


Fig. 1. (a) Physical Situation. (b) Two Segments of the Segmented Conductors' Structure

A. Basic Assumptions

The system is assumed to be a network of connected or disconnected straight cylindrical metallic conductors with arbitrary orientation and finite conductivity. The conductors are subject to the thin-wire approximation, assuming that conductor radius is much smaller than the wavelength and the wire length is much greater than the radius. This assumption enables to approximate the total current in the conductors as filamentary line current in the conductors' axis. Also the current on open end points is assumed to be zero. Conductors can be below, above or penetrate the earth's surface. The soil is modeled as linear and homogeneous half-space characterized by conductivity, permittivity and permeability constants.

B. Approximation of the Longitudinal Current

First a set of current sampling points along the conductors' network is defined, Fig. 1 (a). Such points are defined at each corner or bending point, at each junction where several conductors intersect and at the conductors end points. These current sampling points divide the network of conductors into a number of fictitious segments. Figure 1 (b) shows two such segments. The longitudinal current $I(\ell)$ at point ℓ is then approximated along the conductors' network by a linear combination of M expansion functions $F(\ell)$:

$$I(\ell) = \sum_{j=1}^M I_j F_j(\ell) \quad (1)$$

Here I_i are unknown current samples and $F_j(\ell)$ are overlapped, so called "sinusoidal" expansion functions, Fig. 2 (b). For example, sinusoidal expansion function illustrated in Fig. 2 (a) is:

$$F(\ell) = \frac{\sinh \gamma_1 (\ell - \ell_1)}{\sinh \gamma_1 d}, \quad \gamma_1^2 = -\omega^2 \mu_1 \epsilon_1, \quad \epsilon_1 = \epsilon_1 + \frac{\sigma_1}{j\omega} \quad (2)$$

Here d denotes the length of the segment, as illustrated in Fig. 2. The constants of conductivity, permittivity and permeability of the medium are denoted by σ_1 , ϵ_1 and μ_1 ,

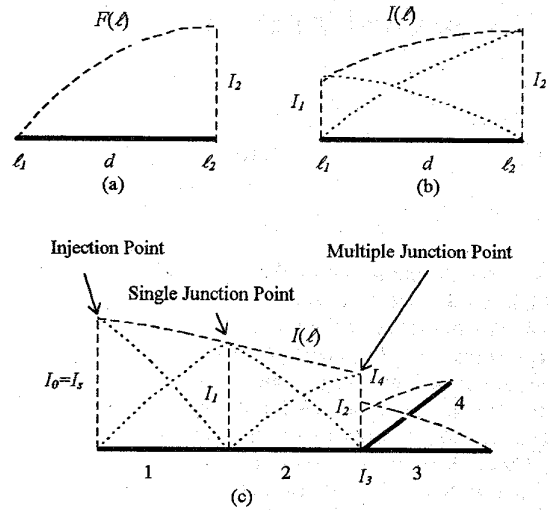


Fig. 2. Approximation of Longitudinal Current. (a) Sinusoidal Function. (b) Two Overlapped Sinusoidal Functions. (c) Current Along Network of Segmented Conductors.

respectively, $j = \sqrt{-1}$ and ω is angular frequency. It should be noted that the time-variation $\exp(j\omega t)$ is suppressed.

Motivation for the choice of expansion functions (2) is given in the next section. It is important to note that segment length d in (2) has to be shorter than the wavelength in the soil (usually six segments per wavelength is acceptable).

The energization of the conductors' network is by injection of current at arbitrary current sampling point. The current at the injection point is equal to the current of the source I_s . The Kirchhoff's current law is explicitly enforced on all segments' junction points, Fig. 2 (c).

Actual number of segments depends on the variation of the current along the conductors and the ability of (1) to approximate accurately the real current distribution.

C. Rigorous Expressions for the Electric Field

The next step in the development of the analytical model is to evaluate electric field at arbitrary observation point radiated by the approximated current distribution.

In this study, the influence of the interface between the air and the earth is taken into account approximately by the modified image theory [12]. Applied expressions are given in Appendix I. By this way the analysis is reduced to homogeneous space, either soil or air, depending on the position of the observation point.

One of the reasons for the choice of the sinusoidal approximating function (2) for currents is that it is probably the only finite line source with simple closed-form expressions for the near fields [13]. The rigorous expres-

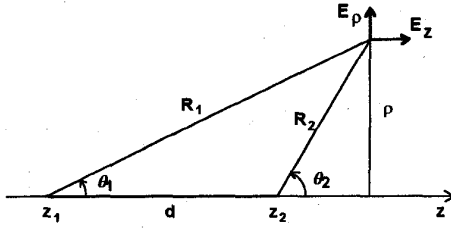


Fig. 3. Local Coordinate System

sions for the ρ - and z -components of the electric field at a near or distant point due to a line current source, in a local cylindrical coordinate system illustrated in Fig. 3, are [14]:

$$E_\rho = \eta_1 \frac{C}{\rho} I [-\exp(-\gamma_1 R_2) \sinh \gamma_1 d - \exp(-\gamma_1 R_1) \cos \theta_1 - \exp(-\gamma_1 R_2) \cosh \gamma_1 d \cos \theta_2] \quad (3)$$

$$E_z = \eta_1 C I \left[-\frac{1}{R_2} \exp(-\gamma_1 R_2) \cosh \gamma_1 d - \frac{1}{R_1} \exp(-\gamma_1 R_1) \right]$$

$$\eta_1 = \sqrt{\frac{\mu_1}{\epsilon_1}}, \quad C = \frac{1}{4\pi \sinh \gamma_1 d}$$

where various quantities are illustrated in Fig. 3 or are given in (2). The sinusoidal current distribution along z is zero at z_1 and at maximum I at z_2 .

The electric field at a point near the grounding system is the sum of contributions from the overlapping sinusoidal current sources in all segments. The derivation of (3) is included in [10]. It should be noted that although only longitudinal current in conductors appears in (3), the contribution of the charge distribution along conductors is also taken into account [10].

D. Evaluation of the Current Distribution

It is necessary to determine M unknown current samples I_j to evaluate the current distribution (1). The current distribution is determined by the electromagnetic interactions between segments. To evaluate these interactions the method introduced by Prof. Richmond [15] may be used. Sinusoidal expansion currents in any two neighbor segments may be considered as electric dipole. Such electric dipoles are typically in V form with each arm extended on one segment. The current is zero at the end points of the segments and rises sinusoidally to a maximum at the junction point of the segments, as illustrated in Fig. 4:

$$I_n^d(\ell_n) = I_n F_n^d(\ell_n) \quad (4)$$

where superscript d denotes distribution along dipole n . Now, the distribution of the current over the conductors'

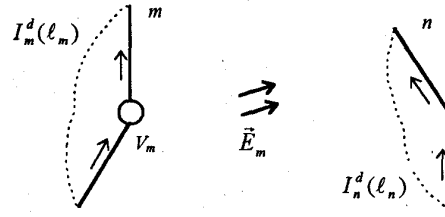


Fig. 4. Evaluation of Mutual Impedance Between Dipoles.

network can be observed as distribution of overlapped dipoles. The only exception is the segment with injection point, where one electric monopole is placed.

Mutual electromagnetic interaction between dipoles can be expressed as mutual impedance obtained by the following fictitious experiment, Fig. 4. We introduce a fictitious ideal voltage generator V_m at the junction point of dipole m . Current distributions $I_m(\ell)$ and $I_n(\ell)$ are induced in the dipoles. Mutual impedance between dipoles m and n , z_{mn} is [16]:

$$z_{mn} = \int_{\ell_n} F_n^d(\ell_n) \bar{\ell}_n \cdot \bar{E}_m d\ell \quad (5)$$

Here $\bar{\ell}_n \cdot \bar{E}_m$ is tangential component of the electric field due to current in dipole m at the surface of the segments of dipole n . The mutual impedance z_{mn} depends only on the geometry of the system, the excitation frequency and the characteristics of the medium. Eq. (5) is valid for lossless conductors. The underlying theory can be found elsewhere [15,16]. Appendix II provides a brief description of the steps involved in the derivation of (5) and the extension for lossy conductors.

Now, the required system of equations can be written:

$$\begin{bmatrix} z_{11} & z_{12} & \cdots & z_{1N} \\ z_{21} & z_{22} & \cdots & z_{2N} \\ \vdots & \vdots & \ddots & \vdots \\ z_{N1} & z_{N2} & \cdots & z_{NN} \end{bmatrix} \begin{bmatrix} I_1 \\ I_2 \\ \vdots \\ I_N \end{bmatrix} = \begin{bmatrix} -z_{10} I_s \\ -z_{20} I_s \\ \vdots \\ -z_{N0} I_s \end{bmatrix} \quad (6)$$

where z_{mn} are elements of the so-called generalized impedance matrix and z_{k0} , $k=1,2,\dots,N$, are mutual impedances between the N dipoles and the "injecting" monopole.

It is important to note that z_{mn} (5) are physically impedances and conform to reciprocity. This is in contrast to methods based on "point matching" [8,17], where corresponding impedances are not reciprocal. As a consequence, the z -matrix in (6) is symmetrical, and only half of the elements have to be evaluated, which contributes to the computational efficiency of this method.

The integral in the right side of (5) can be solved by closed-form expressions [18]. These involve exponential integrals that can be solved without numerical integra-

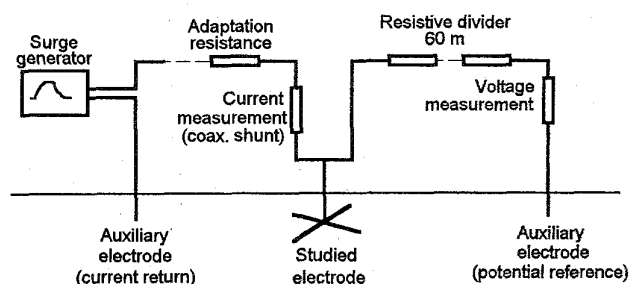


Fig. 5. Measuring set-up (from [19]).

tion, which also contributes to the accuracy and computational efficiency of this method. Also, the sinusoidal expansion functions can better approximate the current along conductors than stepwise approximation [8], which results in smaller number of segments and consequently in smaller system of equation (6).

E. Electromagnetic Fields, Leakage Currents, Voltages, and Impedance to Ground

Once the current distribution along the conductors' network (1) has been computed, the electric field (3) can be calculated at any point by summing the contributions due to the currents in each segment. The leakage current density can be evaluated as the product of the normal component of the electric field at the surface of a ground conductor and conductance of the soil [8]. Voltages between two points along a given path can be evaluated as the line integral of the electric field vector [9]. Impedance to ground can be evaluated as a ratio between the voltage from feed to remote point and the injecting current [8].

It should be noted that the concept of potential, widely used in low frequency grounding system analysis, can lead to difficulties in higher frequency or transient analysis. It is well known that voltage is uniquely defined in static case and it is equal to potential difference, but it is not so in general case [1]. It is important that voltage for the higher frequencies is usually dependent on the path of integration of the electric field. The path dependence of voltage is further discussed in Appendix III.

III. VERIFICATION OF THE COMPUTER MODEL

A. Comparison with Field Measurements by EDF

Recordings from extensive field measurements of transient voltages to remote ground performed by the Electricite de France (EDF) are used to verify the model. Impulse currents have been fed into single- and multi-conductor grounding arrangements and resulting transient voltage to remote ground has been measured by means of a 60 m long ohmic divider with measuring bandwidth of 3 MHz [19].

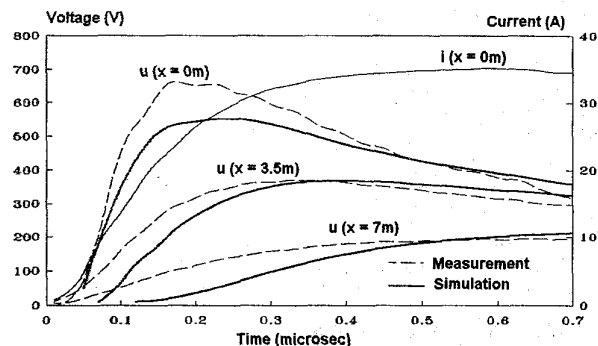


Fig. 6. Measured and computed transient voltage to ground at three points along horizontal copper wire (15 m length, 12 mm radius, 0.6 m depth, 70 Ω m soil's resistivity, 15 soil's relative permittivity).

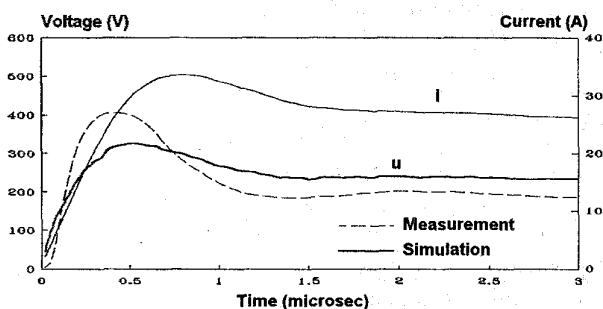


Fig. 7. Measured and computed transient voltage to ground of vertical steel rod (6 m length, 16 mm diameter, 50 Ω m soil's resistivity, 15 soil's relative permittivity).

Figure 5 provides only a simple illustration of the measuring set-up. Surge generator with a peak value of 20 kV was connected to the investigated electrode with a conductor, which was insulated from ground and adapted to the surge generator's characteristic impedance ($Z_c \cong 500 \Omega$). The resulting current impulses had peak values about 30 A and rise times adjustable from 0.2 to 3 μ s. To avoid stationary waves generated on high frequencies, the investigated electrode was connected to the potential reference auxiliary electrode by a voltage divider with high voltage (HV) arm of sufficient length (60 m). The HV arm was composed of a series of ceramic resistances connected to very short connectors. By employing this measuring arrangement a constant transfer function in the measuring bandwidth could be realized. The model soil resistivity was measured separately. Interested reader is referred to numerous publications by the EDF (for example [20]) for more details on the measurements.

Figure 6 shows the oscillograms of recorded current impulse injected in the beginning point of 15 m long horizontal ground wire and transient voltage to remote ground at three points along the wire. The first point is at the beginning of the wire, the second is at 3.5 m distance from the beginning of the wire and the third is at 7 m

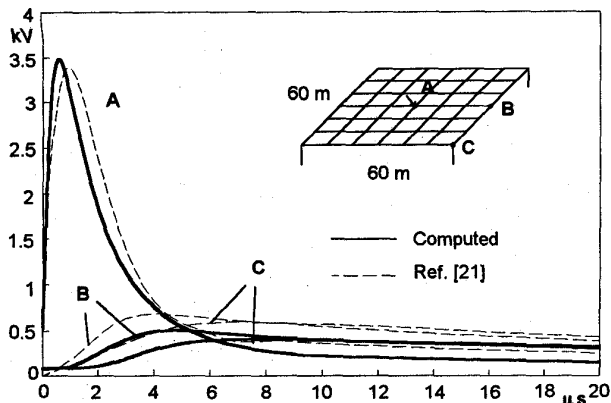


Fig. 8. Transient Voltage Response of 60m x 60m Grounding Grid to a $1/20 \mu\text{s}$ 1 kA Crest Surge. Comparison with Ref. [21]. (6 by 6 10m square meshes, 10m ground rods, 0.6 m depth, 2/0 copper conductor, 100 $\Omega\text{-m}$ soil's resistivity, 36 soil's relative permittivity).

distance from the beginning of the wire. Voltages to remote ground are computed by the computer program integrating the electric field from the surface of the conductor to the neutral ground along a horizontal path of integration perpendicular to the axis of the conductor.

Figure 7 shows the oscillograms of recorded current impulse injected in 6 m long vertical ground rod and the recorded and computed transient voltage to remote ground at the injection point.

The measured voltages are always higher during the current rise than the corresponding values of the computation. Such tendency was also observed when another analytical model, based on transmission line theory and EMTP [10], was validated in EDF at Paris, France. It was concluded in [23] that the measured voltages are likely to be amplified by some remaining inductive voltage drop during the wave front along the divider that is added to the actual potential rise at the clamp of the ground conductors. It should be noted that the presented results of the computations are only voltages to neutral ground of points at the surface of the buried conductor. The connecting conductors and the measurement circuit with the 60 m long voltage divider were not included in the simulation.

B. Comparison with Other Published Results

The results from the presented computer model are compared with other authors' model [6,21]. Figure 8 presents transient voltage response of the illustrated 60m x 60m grid with 10m ground rods in the corners, subjected to $1/20 \mu\text{s}$ 1 kA crest current surge injected at the middle point of the grid. Transient voltages at the feeding point A, middle side point B and corner point C are presented. Results from [21] are illustrated with broken lines and

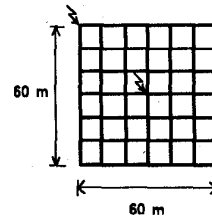


Fig 9. Grounding Grid Adopted for Computations.

computed results are illustrated with full lines. Good agreement is reached for the transient voltages at the feeding point, with small shift forward in time for the results from [21]. On the other side, model from [6,21] tends to overestimate voltages at the edge of the grid in comparison with here computed results. This may be related to the quasi-static approximation used in [6,21] that introduce error in the transient voltage computations on larger distances when impulse contains higher frequencies. Such distances may become comparable to the dimensions of the grid in more conductive soil.

Also, the results from the previous more simplified version of the presented model [9], have been compared with other independent model [11] for 60m x 60m grounding grid given in Fig. 9. The good agreement between the compared results has been reported.

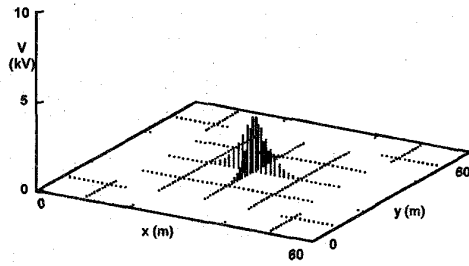
IV. EXAMPLE OF APPLICATION: TRANSIENT VOLTAGES TO REMOTE GROUND OF GRID CONDUCTORS

60m x 60m grounding grid with 6 by 6 10 meter square meshes constructed of copper conductors with diameter 1.4 cm, buried at 0.5 m depth, is illustrated in Fig. 9. Soil is homogeneous with resistivity 100 $\Omega\text{-m}$ and relative permittivity 36. Concerning the injection of the current, two scenarios are considered: the first one is with injection of the current in the corner point of the grid and, alternatively, the second one in the middle point, Fig. 9. A typical double-exponential current impulse, with peak value 1 kA, time-to-maximum 1 μs and time-to-half-maximum 50 μs , is fed to the grid:

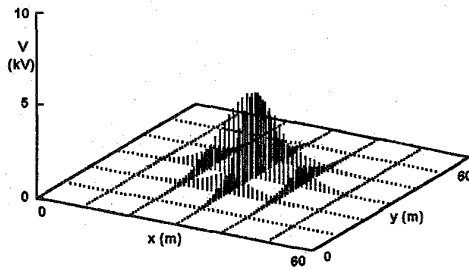
$$i(t) = I(e^{-\alpha t} - e^{-\beta t}) \quad (7)$$

where $I = 1.0167$ kA, $\alpha = 0.0142 \mu\text{s}^{-1}$, $\beta = 5.073 \mu\text{s}^{-1}$, and $i(t)$ and t are in (kA) and (μs), respectively.

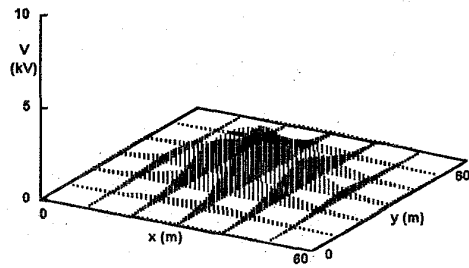
Figures 10 and 11 show the temporal and spatial distribution of the voltages to remote ground of grid conductors. The spatial distributions are presented in compact 3D graphical form and temporal variations are presented as individual "snapshots" of the computer animation. Such presentation enables instant global insight in the distribution of voltages on large grids during the transient period.



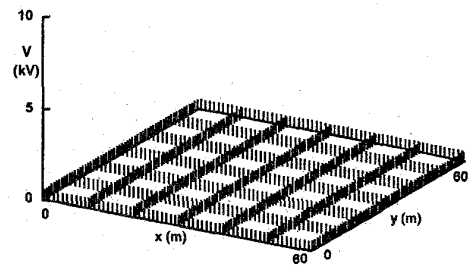
$t = 0.1 \mu s$



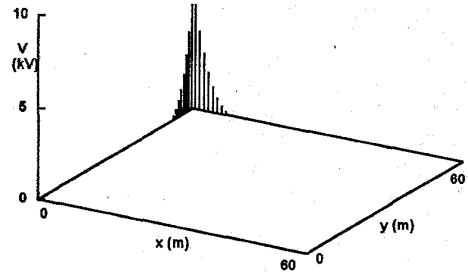
$t = 0.5 \mu s$



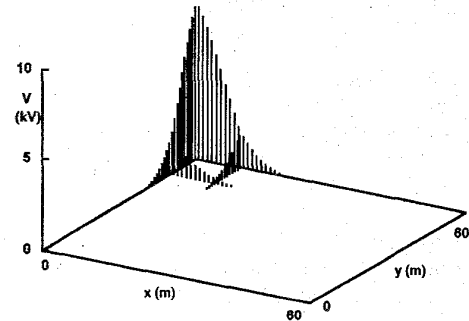
$t = 1 \mu s$



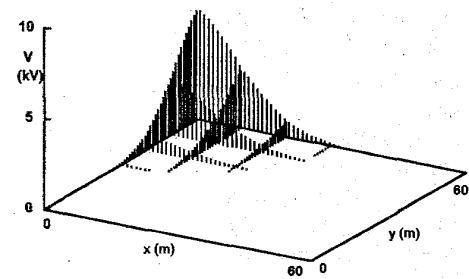
$t = 10 \mu s$



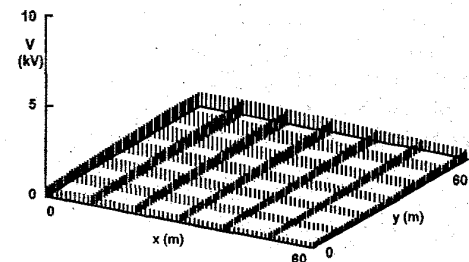
$t = 0.1 \mu s$



$t = 0.5 \mu s$



$t = 1 \mu s$



$t = 10 \mu s$

Fig. 10. Transient Voltages to Remote Ground of 60m x 60m Grid Conductors for Current Impulse Injected in the Middle Point.

Fig. 11. Transient Voltages to Remote Ground of 60m x 60m Grid Conductors for Current Impulse Injected in the Corner.

Presented results show large differences of the voltage to remote ground between points on the grid conductors in the first few μs of the transient response. High values of the voltage occur at grid conductors near the injecting point and are further spreading toward the rest of the grid while the values are decreasing. Transient voltage responses are impulses that lead the injected current impulse. For example, maximum values of the voltages near the feed point occur as early as $0.3 \mu\text{s}$ from the beginning of the excitation, compared to time-to-maximum of $1 \mu\text{s}$ of current impulse, for the presented example. The transient period lasts up to about $8 \mu\text{s}$ for central and $15 \mu\text{s}$ for corner injection, and after that time the voltages are equalized on the whole surface of the grid.

During the transient period, especially during the first few μs , large voltages between points on the grid conductors near the injection point can be estimated. It is important that such large voltages are observed even between near points in the same mesh (Fig. 10 for $t = 0.5 \mu\text{s}$), when the lightning current is fed there. As expected, voltages are considerably higher for injection at the edge of the grid. It should be noted that the computed values are normalized to 1 kA peak value of the injected current impulse and will be proportionally larger for higher currents. Also voltages will be larger in poorly conductive soil.

Presented computer model can be used in EMC and lightning protection studies where detailed estimation of voltage fluctuations on the surface of the grounding grid is of interest. It may be used first to acquire a global view of the spatial and temporal voltage distributions and next for detailed computations of voltages between specified points along given paths.

V. DOMAIN OF APPLICABILITY

Main limitations in the use of the described computer model are set by the application of the modified image theory and the neglect of the soil ionization.

The modified image theory limits the frequency and the position of the field observation points. Direct comparison with the more accurate model [8] shows that the computations of voltages are in good agreement for frequencies lower than few MHz, which is suitable for analysis of the response to typical lightning current impulses, with rise time of about or longer than $1 \mu\text{s}$. Also, the results are in good agreement if at least one of the points, between which the voltage is computed, is near the grid conductors. An example of such "near" points are at the surface of the ground above the grid.

The neglect of the soil ionization limits the peak value of the excitation current impulse that can be analyzed. It has been shown that it is highly probable that soil ioniza-

tion will occur in large grounding systems in case of lightning [22]. Therefore, in cases when high current impulses are concerned, it is necessary to compute the electric field at the surface of the grid conductors and check if the soil ionization threshold is met or exceeded.

The computer program is computationally more efficient than the more accurate model [8] and requires a fraction of computer time reported in [8].

VI. CONCLUSIONS

A computer model for time-harmonic and transient voltages between points at or near buried and above ground network of conductors is presented. The model is based on the electromagnetic field theory approach and includes several improvements over the previous models, such as:

- better approximation of the current distribution in grid conductors,
- rigorous formulas for electric fields,
- evaluation of the electromagnetic interactions between parts of the system based on sound physical approach and closed-form expressions.

Voltages between two points are computed rigorously including the dependence on the path of integration. The applied accurate model enables computations of voltages between points at the surface of the grid conductors. The computer model is validated by comparison with field measurements by EDF. The domain of applicability is limited by the modified image theory and the neglect of the soil ionization, but the model is suitable for analysis of responses to typical lightning current impulses.

As an example, spatial distributions of transient voltages to remote ground of points at the surface of $60\text{m} \times 60\text{m}$ grounding grid conductors are presented. The spatial distributions are presented in compact 3D graphical form and time variations are presented as individual "snapshots" of computer animation. Large differences of the voltages to remote ground even between near points in one mesh are observed during the early time of the transient response especially near the feed point of the lightning current impulse.

The presented computer model can help in EMC and lightning protection studies that require more detailed knowledge of the spatial and temporal distribution of voltages in large grounding systems.

VII. ACKNOWLEDGMENT

The work was supported in part by the Ministry of Science of the Republic of Macedonia.

VIII. REFERENCES

- [1] S. Benda, "Earthing and Bonding in Large Installations", *ABB Review*, No. 5, 1994, pp. 22-29.
- [2] A.L. Vainer, "Impulse Characteristics of Complex Earthings", *Elektrichestvo*, No. 3, 1966, pp. 23-27, (in Russian).
- [3] B.R. Gupta and B. Thapar, "Impulse Impedance of Grounding Grids", *IEEE Transactions on Power Apparatus and Systems*, Vol. PAS-99, Nov./Dec. 1980, pp. 2357-2362.
- [4] R. Verma and D. Mukhedkar, "Fundamental Considerations and Impulse Impedance of Grounding Grids", *IEEE Transactions on Power Apparatus and Systems*, Vol. PAS-100, March 1981, pp. 1023-1030.
- [5] A.P. Meliopoulos and M.G. Moharam, "Transient Analysis of Grounding Systems", *IEEE Transactions on Power Apparatus and Systems*, Vol. PAS-102, Feb. 1983, pp. 389-399.
- [6] A.D. Papalexopoulos and A.P. Meliopoulos, "Frequency Dependent Characteristics of Grounding Systems", *IEEE Transactions on Power Delivery*, Vol. PWRD-2, October 1987, pp. 1073-1081.
- [7] M. Ramamoorthy, M.M.B. Narayanan, S. Parameswaran, and D. Mukhedkar, "Transient Performance of Grounding Grids", *IEEE Transactions on Power Delivery*, Vol. PWRD-4, Oct. 1989, pp. 2053-2059.
- [8] L. Grcev and F. Dawalibi, "An Electromagnetic Model for Transients in Grounding Systems", *IEEE Transactions on Power Delivery*, Vol. PWRD-5, No. 4, October 1990, pp. 1773-1781.
- [9] L. Grcev, "Computation of Transient Voltages Near Complex Grounding Systems Caused by Lightning Currents", *Symposium Record of the IEEE 1992 International Symposium on Electromagnetic Compatibility*, 92CH3169-0, pp. 393-400.
- [10] F. Menter and L. Grcev, "EMTP-Based Model for Grounding System Analysis", *IEEE Transactions on Power Delivery*, Vol. 9, October 1994, pp. 1838-1849.
- [11] W. Xiong and F. Dawalibi, "Transient Performance of Substation Grounding Systems Subjected to Lightning and Similar Surge Currents", *IEEE Transactions on Power Delivery*, Vol. 9, July 1994, pp. 1421-1427.
- [12] T. Takashima, T. Nakae, and R. Ishibashi, "Calculation of Complex Fields in Conducting Media", *IEEE Transactions on Electrical Insulation*, Vol. 15, 1980, pp. 1-7.
- [13] S.A. Schelkunoff and H.T. Friis, *Antennas, Theory and Practice*, New York: John Wiley & Sons, 1952, p. 401.
- [14] D.V. Otto and J.H. Richmond, "Rigorous Field Expressions for Piecewise-Sinusoidal Line Sources", *IEEE Transactions on Antennas and Propagation*, Vol. AP-17, January 1969, p. 98.
- [15] J.H. Richmond, "Radiation and Scattering by Thin-Wire Structures in the Complex Frequency Domain", in *Computational Electromagnetics*, E.K. Miller, Ed., New York: IEEE Press, 1992.
- [16] W.L. Stutzman and G.A. Thiele, *Antenna Theory and Design*, New York: John Wiley & Sons, 1981.
- [17] F. Dawalibi and A. Selby, "Electromagnetic Fields of Energized Conductors", *IEEE Transactions on Power Delivery*, Vol. 8, No. 3, July 1993, pp. 1275-1284.
- [18] C.W. Chuang, J.H. Richmond, N. Wang, and P.H. Pathak, "New Expressions for Mutual Impedances of Nonplanar-Skew Sinusoidal Monopoles", *IEEE Transactions on Antennas and Propagation*, Vol. 38, No. 2, February 1990, pp. 275-276.
- [19] H. Rochereau, "Response of Earth Electrodes when Fast Fronted Currents are Flowing Out", *EDF Bulletin de la Direction des Etudes et Recherches*, serie B, no. 2, 1988, pp. 13-22.
- [20] R. Fieux, P. Kouteynikoff, and F. Villefranque, "Measurement of the Impulse Response of Groundings to Lightning Currents", *Proceedings of 15th International Conference on Lightning Protection (ICLP)*, Uppsala, Sweden, 1979.
- [21] A.D. Papalexopoulos, "Modeling Techniques for Power System Grounding Systems", Ph.D. dissertation, Georgia Institute of Technology, Georgia, 1985, (Available from University Microfilms, Ann Arbor, Mich.)
- [22] L. Grcev, "Analysis of the Possibility of Soil Breakdown due to Lightning in Complex and Spacious Grounding Systems", *Proceedings of 22nd International Conference on Lightning Protection (ICLP)*, Budapest, Hungary, September 19-23, 1994, R 3a-07.
- [23] H. Rochereau, "Application of the Transmission Lines Theory and EMTP Program for Modelisation of Grounding Systems in High Frequency Range", *Collection de notes internes de la Direction des Etudes et Recherches*, 93NR00059, 1993, p.21.
- [24] V.H. Rumsey, "Reaction Concept in Electromagnetic Theory", *Physical Review*, Vol. 94, Ser. 2, 1954, pp. 1483-1491.
- [25] R.F. Harrington, *Field Computation by Moment Methods*, New York: IEEE Press, 1993.
- [26] S.A. Schelkunoff, "On Diffraction and Radiation of Electromagnetic Waves", *Physical Review*, Vol. 56, August 1939.
- [27] E.C. Jordan and K.G. Balmain, *Electromagnetic Waves and Radiating Systems*, New Jersey: Prentice-Hall, 1968.
- [28] J.A. Stratton, *Electromagnetic Theory*, New York: McGraw-Hill, 1941.
- [29] J.H. Richmond, "Radiation and Scattering by Thin-Wire Structures in a Homogeneous Conducting Medium", *IEEE Transactions on Antennas and Propagation*, Vol. 22, No. 3, March 1974, pp. 365.
- [30] S. Ramo, J.H. Whinnery, and T. Van Duzer, *Fields and Waves in Communication Electronics*, New York: Wiley, 1965.

APPENDIX I - MODIFIED IMAGE THEORY

The electric field radiated by a current element placed above or below the earth's surface can be evaluated by the modified method of images [12]. The following four cases can be considered for the position of the current element and the observation point:

1) *Current source and observation point in soil:* The electric field can be evaluated as a sum of the field of the current source I and its image I' :

$$I' = \frac{\epsilon_1 - \epsilon_0}{\epsilon_1 + \epsilon_0} I \quad (\text{A-1})$$

where ϵ_0 is permittivity of vacuum and ϵ_1 is given in (2).

2) *Current source and observation point in air:* The electric field can be evaluated as a sum of the field of the current source I and its image I' :

$$I' = \frac{\epsilon_0 - \epsilon_1}{\epsilon_1 + \epsilon_0} I \quad (\text{A-2})$$

3) *Current source in soil and observation point in air:* The electric field can be evaluated as field due to the modified current source I'' :

$$I'' = \frac{2\epsilon_0}{\epsilon_1 + \epsilon_0} I \quad (\text{A-3})$$

4) *Current source in air and observation point in soil:* The electric field can be evaluated as field due to the modified current source I'' :

$$I'' = \frac{2\epsilon_1}{\epsilon_1 + \epsilon_0} I \quad (\text{A-4})$$

APPENDIX II - ELEMENTS OF THE GENERALIZED IMPEDANCE MATRIX FOR LOSSY CONDUCTORS

The mathematical formulation is based on physical concept of reaction. Reaction is introduced by Rumsey [24] as a physical observable, such as, for example: mass, length, charge, etc. It is basically a measure of the coupling between two sources. If we view the induced current

$I_n^d(\ell_n)$ in Fig. 4 as one source, then the impedance matrix elements given by (5) may be interpreted as the coupling between this source and the field \vec{E}_m from the current $I_m^d(\ell_m)$ [16].

In the general case the total field (\vec{E}, \vec{H}) can be considered as the sum of an impressed field (\vec{E}', \vec{H}') , generated by independent sources, and a scattered field (\vec{E}^s, \vec{H}^s) , generated by the induced sources by the impressed fields [25]. According to the surface equivalence theorem [26], the conductors may be replaced with the ambient medium, if suitable electric and magnetic current densities (\vec{J}_s, \vec{M}_s) are introduced on the surface S of the conductors. These surface sources do not disturb the existing field anywhere in the exterior region, but generate a null field in the interior region of the conductors. Let us place electric and magnetic current density (\vec{J}_n, \vec{M}_n) in the interior region of the conductors of the n^{th} dipole and test their coupling or reaction with the other sources [16]:

$$\iint_{S_n} (\vec{J}_n \cdot \vec{E}' - \vec{M}_n \cdot \vec{H}') dS + \iint_{S_n} (\vec{J}_n \cdot \vec{E}^s - \vec{M}_n \cdot \vec{H}^s) = 0 \quad (\text{A-5})$$

$$n = 1, 2, 3, \dots, N$$

If field from the sinusoidal expansion functions $F_m(\ell_m)$ (2) of the current in m^{th} dipole is denoted by $(\vec{E}_m^s, \vec{H}_m^s)$, then the general mn^{th} element in the generalized impedance matrix may be written:

$$z'_{mn} = \iint_{S_n} (\vec{J}_n \cdot \vec{E}_m^s - \vec{M}_n \cdot \vec{H}_m^s) dS \quad (\text{A-6})$$

where S_n is the surface of the conductors of the n^{th} dipole. On the perfectly conducting conductor, the magnetic current density \vec{M}_s vanishes, and (5) follows from (A-6).

When conductors have finite conductivity, the tangential electric field at the surface of the conductors can be related to the equivalent electric surface current density

$$\vec{E} = Z_s \vec{J}_s \quad (\text{A-7})$$

where Z_s is the surface impedance defined in [27] as the ratio of the tangential electric field strength at the surface of the conductor to the current density which flows as a result of that tangential electric field. If σ_2 , ϵ_2 and μ_2 represent the common conductance, permittivity and permeability of the conductors, then [28]:

$$Z_s = \frac{\lambda_2}{2\pi a(\sigma_2 + j\omega\epsilon_2)} \frac{J_0(\lambda_2)}{J_1(\lambda_2)} \quad (\text{A-8})$$

Here $\lambda_2 \approx \omega^2(\mu_2\epsilon_2 - \mu_1\epsilon_1)$ and a is the radius of the conductor segment. The Bessel functions of the first kind of order zero and one are denoted J_0 and J_1 , respectively.

Using $\vec{M}_s = \vec{E} \times \vec{n}$ and $\vec{J}_s = \vec{I}(\ell) / 2\pi a$, it follows:

$$\vec{M}_s = Z_s \vec{J}_s \times \vec{p} = \vec{\phi} Z_s I(\ell) / 2\pi a \quad (\text{A-9})$$

Applying reciprocity to (A-6) and substituting (A-9) in (A-6) leads to [16]:

$$z'_{mn} = \int_{\ell_n} F_n^d(\ell_n) [\vec{\ell}_n \cdot \vec{E}_m - Z_s \vec{\phi}_n \cdot \vec{H}_m] d\ell \quad (\text{A-10})$$

Applying Ampere's law $\vec{\phi}_n \cdot \vec{H}_m = I_m(\ell_m) / 2\pi a$ and substituting in (A-10) it follows:

$$z'_{mn} = z_{mn} - \frac{Z_s}{2\pi a} \int_{(m,n)} F_m^d(\ell_m) F_n^d(\ell_n) d\ell \quad (\text{A-11})$$

where z_{mn} is given in (5) and region (m,n) are segments shared by dipoles m and n . FORTRAN subroutines for (A-11) are also available [29].

APPENDIX III - ESTIMATION OF PATH DEPENDENCE OF VOLTAGE

It is well known that the voltage between points 1 and 2 along a path ℓ_{12} in general case is defined by [30]:

$$V_{12} = \int_{\ell_{12}} \vec{E} \cdot d\vec{\ell} = (\Phi_1 - \Phi_2) - \frac{\partial}{\partial t} \int_{\ell_{12}} \vec{A} \cdot d\vec{\ell} \quad (\text{A-12})$$

where Φ_1 and Φ_2 are values of the scalar potential at points 1 and 2, and \vec{A} is the vector potential. For static fields, the last term is zero and the voltage is exactly the difference of the scalar potentials. For time-varying fields, voltage in general depends on the path taken between two specified points.

The path dependence of voltage may be estimated by the following formula based on Faraday's law:

$$V'_{12} - V_{12} = -\frac{\partial}{\partial t} \int_S \vec{B} \cdot d\vec{S} \quad (\text{A-13})$$

where V'_{12} and V_{12} are voltages computed along different paths, and S is the surface bounded by these paths. So the voltages defined along the two paths will be different whenever there is any time-varying magnetic flux enclosed between the two paths [30].

Dr. Leonid Greev (M'84) was born in Skopje, Macedonia, on April 28, 1951. He received Dipl. Ing. degree from the University of Skopje, and the M.Sc. and Ph.D. degrees from the University of Zagreb, Croatia, all in Electrical Engineering, in 1978, 1982 and 1986, respectively.

From 1978 to 1988, he held a position with the Electric Power Company of Macedonia, Skopje, working in the Telecommunications and later in the Information System Department. He worked on a number of projects involving telecommunications systems, and electromagnetic compatibility related problems. He also worked on development of specialized computer software. He was a Head of the Information System Department from 1985 during its formation. In 1988, he joined the Faculty of Electrical Engineering at the University of Skopje, and is now an Associate Professor of Electrical Engineering. His present research interests are in computational electromagnetics applied to transients, grounding and interference.

Dr. Leonid Greev is a member of IEEE PE, AP, MTT, EMC, and MAG Societies. He is also a member of the Applied Computational Electromagnetic Society.